

LRP 697/01

May 2001

**Plasma Shape Effects on  
Sawtooth/Internal Kink Stability and  
Plasma Shaping Using  
EC Wave Current Profile Tailoring in TCV**

A. Pochelon, F. Hofmann, H. Reimerdes, C. Angioni,  
R. Behn, R. Duquerroy, I. Furno, T.P. Goodman,  
P. Gomez, M.A. Henderson, An. Martynov, P. Nikkola,  
O. Sauter, A. Sushkov

Accepted for publication in  
NUCLEAR FUSION

(extended version of paper EXP 3/10,  
18<sup>th</sup> IAEA Fusion Energy Conference,  
Sorrento, Italy, 2000)

# Plasma Shape Effects on Sawtooth / Internal Kink Stability and Plasma Shaping Using EC Wave Current Profile Tailoring in TCV

A. Pochelon, F. Hofmann, H. Reimerdes, C. Angioni, R. Behn, R. Duquerroy, I. Furno, T.P. Goodman, P. Gomez, M.A. Henderson, An. Martynov, P. Nikkola, O. Sauter, A. Sushkov

Centre de Recherches en Physique des Plasmas, Ecole Polytechnique Fédérale de Lausanne, Association EURATOM-Confédération Suisse, CH-1015 Lausanne EPFL, Switzerland

\*RRC, Kurchatov, Russia

e-mail contact of main author: Antoine.Pochelon@epfl.ch

**Abstract.** This paper addresses the effect of plasma shaping (triangularity and elongation) on the sawtooth stability as well as the technique of current profile broadening using off-axis electron cyclotron heating (ECH) to enlarge the operational range towards higher elongations. The plasma shape strongly influences the sawtooth period and amplitude. This effect is emphasised by ECH, with the sawtooth period becoming shorter at low triangularity or at high elongation; for these plasma shapes, the pressure profile inside  $q=1$  remains essentially flat throughout the sawtooth cycle. A comparison of the sawtooth response with marginal Mercier stability shows that the critical pressure gradient at  $q=1$  is particularly low for plasma shapes where the increased sawtooth repetition frequency prevents the peaking of the pressure profiles. For these shapes, the ideal internal kink is also found unstable from stability calculations. The stability of highly elongated plasmas depends largely on current profiles. The operational range at low current has been extended towards higher elongation using ECH heated discharges. Far off-axis second harmonic X-mode ECH power deposition proves to be an efficient tool for current profile tailoring allowing a significant elongation increase at constant quadrupole field.

## 1. Introduction

Plasma shaping is one of the means by which tokamak plasma performance can be improved. The increase of plasma elongation allows an important increase of the plasma current at a fixed toroidal magnetic field, which is favourable for the confinement time, as the usual confinement scaling laws exhibit an improvement of confinement with plasma current. Elongation also improves the maximum normalised pressure  $\beta_N$ , which scales with plasma current. Plasma shaping has also an influence on MHD properties: it has been found recently that triangularity and elongation modify profoundly the sawtooth activity behaviour, shown to be governed by Mercier and internal kink stability [1]. This paper extends previous experimental results on the effect of shape on sawteeth with central ECH, studied at elongations  $\kappa \leq 2.1$ , up to very high elongations,  $\kappa < 2.8$ , albeit only in the ohmic regime so far.

Very high elongation plasmas ( $2.2 < \kappa < 2.8$ ) in TCV were first created in ohmic, low  $q$ , high current discharges [2]. Low  $q$  discharges were a necessary ingredient for axis-symmetric mode stability by providing sufficient current density close to plasma edge. This constrained the ohmic results to a range of normalised currents,  $I_N = I/aB \sim 2.8-3.5$  MA/mT, close to the  $\beta$ - or the current-limit. For confinement and pressure limit studies at these extreme elongations, it is necessary to develop discharges at lower  $I_N$ , since the maximum  $\beta_N$  is predicted around  $I_N \sim 2$ . At such a reduced current, the discharges are no longer vertically stable at these elongations. It is therefore necessary to find means of broadening the current profile. This paper describes the development of low  $I_N \sim 1$ , high  $q$  discharges  $q \sim 12$ , using off-axis EC waves to broaden the current profile in quasi-steady state, that is without making use of the current ramp-up transient. This is the first time that current profile tailoring is used explicitly to obtain stable high elongation discharges.

The TCV tokamak ( $R=0.88$  m,  $a=0.25$  m,  $I_p \leq 1$  MA,  $B < 1.54$  T,  $\kappa < 2.8$ ,  $-0.7 < \delta < 0.9$ ) is particularly suited for the development of various and extreme plasma shapes and for the study of shape related issues. It is presently equipped with a total of 3 MW ECRH/ECCD power at the second harmonic (X2), 82.7 GHz, injected by 6 independent launchers. The launchers can be steered during the discharge, which allows both for highly localised power deposition schemes and for the follow-up of an expanding discharge, e.g. by imposing the deposition at a constant normalised radius [3].

## 2. Dependence of sawtooth / Internal kink stability on plasma shape

### 2.1 Triangularity and elongation effects with central ECH

In the TCV tokamak the sawtooth period and the sawtooth amplitude are observed to depend strongly on the shape of the poloidal plasma cross-section. Systematic scans of plasma elongation and triangularity ( $0 < \delta < 0.5$ ,  $1.2 < \kappa < 2.1$ ) show small sawteeth with short periods at high elongation or at low and negative triangularity, and large sawteeth with long periods at low elongation or high triangularity. Additional central electron cyclotron heating power further amplifies the shape dependence of the sawtooth properties. The sawtooth period can either increase or decrease with additional heating power depending on the plasma shape. As an example, Fig. 1 shows the increase of the sawtooth period with power deposited inside the  $q=1$  surface at high triangularity and the decrease at low triangularity. Similarly, the sawtooth period decreases for high elongations [1].

An analytic expansion of the Mercier criterion [4] suggests that low triangularity and high elongation lead to a lower ideal MHD central pressure limit, as shown in Fig. 2 for the shape parameters of the  $q=1$  surface. These analytic results are confirmed by ideal MHD calculations using the KINX code [5], which show that the internal kink mode is unstable for the lowest triangularity and highest elongation cases of Fig. 2, and stable for the highest triangularity and lowest elongation cases. Therefore, for plasma shapes where additional heating and, consequently, increased central pressure gradients shorten the sawtooth period, the low central pressure gradient limit achieved is consistent with ideal MHD predictions of internal kink stability. This central pressure gradient limitation can be expressed by a limitation of the poloidal beta on the  $q=1$  surface, the beta Bussac (see e.g. [1]):  $\beta_{p,1} = (\langle p \rangle_1 - p(\rho_1)) / (B_p^2(\rho_1) / 2\mu_0)$ , where  $\langle p \rangle_1$  denotes a volume average within the  $q=1$  surface  $\rho_1$  and  $p(\rho_1)$  the pressure at this surface, so that the numerator represents the volume averaged incremental pressure above the pressure at  $q=1$ . In addition, the experimentally observed sawtooth behaviour is consistent with a sawtooth trigger model, which assumes the ideal or resistive internal kink to be responsible for the sawtooth crash [6]. The results of Fig. 1 exhibit two triangularity ranges: for  $\delta \leq 0.2$ , where the sawtooth period decreases with power in accordance with the destabilising effect of central pressure on internal kink stability; and for  $\delta \geq 0.3$ , for which the increased pressure gradients are stabilising, e.g. by diamagnetic effects [6].

Ideal KINX code results also show the internal kink stability to be dependent on shape parameters: the ideal internal kink is more stable at larger triangularities  $|\delta_1|$ , as shown for large aspect ratio in [7]. At large  $|\delta_1|$ , the internal kink mode becomes stable. In the case of a lower TCV-like aspect ratio, this trend is still perceptible, although weaker. In the TCV experiment, the domain of  $|\delta_1|$  over which  $\tau_{ST}$  was investigated is within this unstable, low  $|\delta_1|$  triangularity range. In the experimental triangularity scan, discharges with a triangularity  $\delta_1 < 0.06$  and with elongation  $\kappa_1 > 1.3$  show indeed a shortening of  $\tau_{ST}$  with  $P_{EC}$  (see Fig. 2).

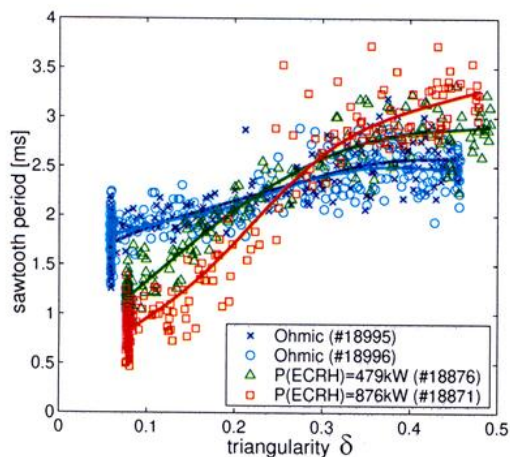


Fig. 1 Sawtooth period as a function of triangularity  $\delta$  for an ohmic discharge with  $\kappa \sim 1.5$  and different ECRH powers injected inside  $q=1$ . The sawtooth period decreases for low triangularity,  $\delta < 0.2-0.3$  and increases above. Electron density and sawtooth inversion radius were kept constant ( $\rho_{inv} \sim 0.5$ ,  $q_{eng} = 5abB/RI_p \sim 2$ ).

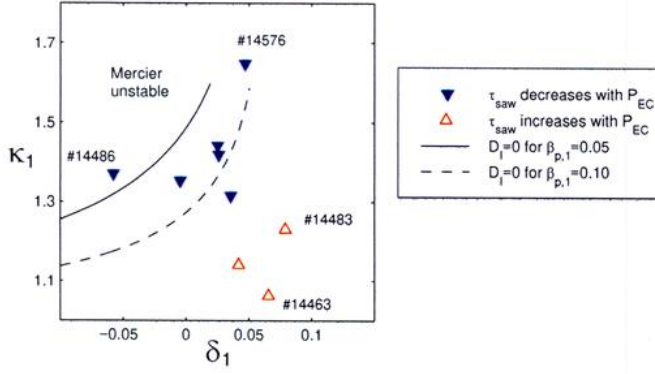


Fig. 2 The discharges of different shapes are shown as a function of triangularity and elongation of the  $q=1$  surface. The plasma shapes are compared to the shapes corresponding to marginal stability according to the Mercier criterion [4] for two different values of  $\beta_{p,1}$  and assuming constant shear  $s_1 = \rho_1(dq/d\rho_1) = 0.1$  and inversion radius  $\rho_{inv} = 0.5$ .

The  $m=1$ ,  $n=1$  mode exponential growth rate  $\gamma$  was directly measured from either magnetic ( $n=1$ ) and/or soft X-ray signals ( $m=1$ ) in JET [8]. In these JET measurements, both  $n=1$  edge magnetic measurements and centre  $m=1$  motion yield proportional displacements and the same growth rate. The growth rate is evaluated at a time when the mode is sufficiently developed above noise level or above other modes to allow for a growth rate determination. The growth rate is measured at the time of the maximum growth rate, i.e. at the time when the mode starts to saturate. Similar growth rate measurements have been repeated in TCV as a function of plasma shape, using a 16 coil toroidal array. In TCV, this  $n=1$  growth rate  $\gamma$  increases with triangularity ( $0 < \delta < 0.5$ ) [9], which appears to be in contradiction with both the Mercier marginal stability and the recent sawtooth period data in TCV [1]. In fact, the measured  $\gamma$  scales with the amplitude of the crash pressure drop [8], which increases with the longer sawteeth at high triangularity in TCV. However, an experimental  $\gamma$  can only be measured in the late non-linear phase of the crash, when its amplitude is sufficiently above noise level, but where it is therefore no more necessarily related to the linear  $\gamma$ , which remains inaccessible below noise level.

## 2.2 Extreme elongation ohmic behaviour ( $2.3 < \kappa < 2.8$ )

Extremely elongated ( $2.3 < \kappa < 2.8$ ) ohmic plasmas have been created in TCV at low  $q$ . In these discharges, the sawtooth period,  $\tau_{ST}$ , decreases with elongation, as shown in Fig. 3, extending earlier results [1, 10] to even higher elongation. While the plasma elongation is ramped-up and -down, the density was not maintained constant, leading to different sawtooth periods in the ramp-up and -down (open triangles). If the sawtooth period is normalised to the density, for instance the density of maximum edge elongation  $n_e(k_{a,max})$ , no hysteresis between ramp-up and ramp-down is found (full triangles). Therefore, the  $\tau_{ST}$  values are not the result of transients. This normalisation is justified by the proportionality  $\tau_{ST} \sim n_e$  found in several tokamaks, e.g. TFR, TCA [11, 12] and confirmed in TCV for different elongations ( $\kappa = 1.6, 2.2$ ), at similar measured inversion radii ( $\rho_{inv} \sim 0.40-0.45$ ) for densities ranging from 2 to 5  $10^{19} \text{ m}^{-3}$ .

When the elongation is increased, see Fig. 3, a first discontinuity is seen at  $\kappa \sim 1.9$ , after which the sawtooth period and relative fluctuation amplitude continue to decrease up to an elongation  $\kappa \sim 2.3-2.6$ , where the sawteeth abruptly disappear below resolution. This abrupt transition occurs at a very precise value of the internal inductance,  $l_i \sim 0.69$  (at low  $q$ , large  $\rho_1$ ), see Fig. 4. The sawtooth inversion radius,  $\rho_{inv}$ , remains approximately constant throughout this transition. It does not vary significantly prior to the transition (typically  $\sim 0.49 \pm 0.03$ ), and may vary somewhat more after the transition, where some small randomly re-occurring sawteeth allow its determination, even below  $l_i \sim 0.69$ . The electron temperature profile remains practically unchanged through the transition. Even without sawteeth, the profile remains flat in the centre and shows a sharp rollover in the  $\rho_{inv}$  region, suggesting that  $\rho_1$  does not change during this transition.

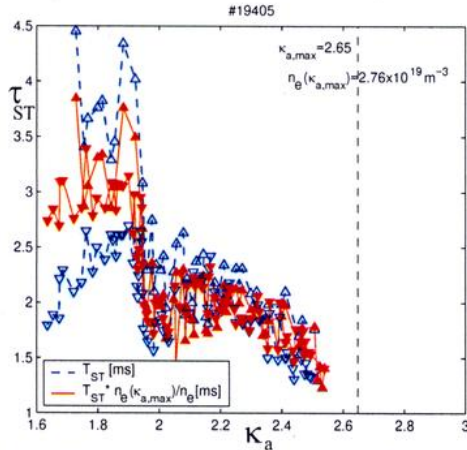


Fig. 3 Decrease of the sawtooth period  $\tau_{ST}$  with elongation and sawtooth disappearance at  $\kappa \sim 2.5$ . The normalisation to  $n_e$  (full triangles) cancels the ramp-up/-down hysteresis (open triangles).

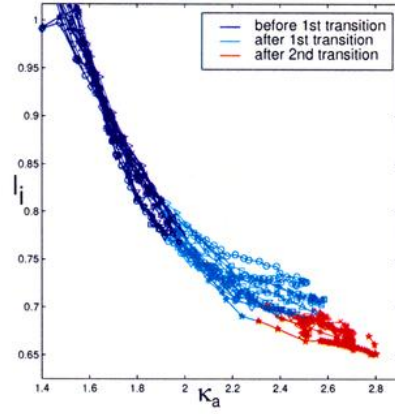


Fig. 4 Abrupt disappearance of sawteeth below an internal inductance of  $l_i = 0.69$  for different  $n_e$  and  $dl_i/dt$ .

Higher toroidal modes,  $n=2, 3, 4$ , measured with magnetic probes, are observed at high elongation, however their exact structure and nature is not yet known. Thus, there are several indications supporting the existence of unstable modes at extreme elongation which flatten the core temperature profile even though the macroscopic sawteeth have disappeared.

### 3. Current profile modifications to increase plasma elongation

The stability of highly elongated plasmas depends largely on current profiles [2]. At high elongation, low current high  $q$  discharges are unstable with respect to axisymmetric modes. We present initial experiments using EC wave current profile broadening to create and stabilise high elongation, low current discharges, which would be ohmically unstable, thus reducing the strong correlation between  $\kappa$  and  $l_i$  in ohmic plasmas at fixed current (Fig. 4).

Among the different EC-schemes, the current profile can be broadened by off-axis ECH, on axis counter-ECCD or off-axis co-ECCD. PRETOR transport code simulations [13, 14] using the local RLW heat transfer coefficients [15] favour off-axis ECH. Let us consider the requirements for maximising the current density in the outer half of the profile. In general, simulations show that the current density  $j(\rho)$  is increased above ohmic at the deposition radius,  $\rho_{dep}$ , and in a layer of finite thickness outside of it. Hence, the optimal  $\rho_{dep}$  to increase  $j(\rho \sim 0.7)$  is typically  $\rho_{dep} \sim 0.7$ . Moving  $\rho_{dep}$  too far in, typically  $\rho_{dep} < 0.5$ , is seen to decrease  $j(\rho \sim 0.7)$ . The experimental task is then the determination of an optimum deposition location in the outer half of the profile, which maximises both elongation and axis-symmetric stability. Central counter-ECCD increases the current in a ring inside  $\rho \sim 0.65$  and decreases it further out, making it less attractive than off-axis ECH, which was also observed experimentally.

The standard EClaunch set-up in these experiments uses 2 to 4 gyrotrons, that is a maximum of 2MW shared between upper lateral and equatorial launchers [3], in off-axis ECH. The discharges are pre-programmed for a constant quadrupole field throughout the ohmic and EC heated phases. Using a high pre-programmed triangularity, similar to that used in ohmic discharges, led to 8% indentation in the mid-plane on the HFS in the EC phase, a wider plasma-wall separation on the LFS and very high central elongation  $k_0 \sim k_{edge}$ . By decreasing the triangularity, the indentation was removed and the elongation on axis reduced, which improves stability and spreads the power more uniformly onto the tiles. This allowed operation at high elongation and low current ( $\kappa=2.4$ ,  $q=13$ ,  $I_p=300kA$ ,  $\langle j \rangle / (q_{0j_0}) \sim 0.22$ ,  $I_N=0.84MA/mT$ ), which would not have been possible with peaked ohmic profiles. As a comparison, ohmic discharges at elongation  $\kappa=2.4$  were typically obtained at current densities which were higher by a factor 2.5.

With an injection of 1.9MW using 4 static EC beams at  $\rho=0.65$  initially, the initial ohmic elongation of 1.75 increases to 2.40 in 0.37s, while the deposition gradually moves to smaller radii,  $\rho=0.5$ . Meanwhile, the internal inductance  $I_i$  decreases from 1.25 to 0.83, which can be attributed to both the increased elongation and the flattened current profile. Open-loop growth rates of the vertical instability, as obtained from a rigid displacement model [16], are  $\gamma_R=996s^{-1}$  in the ohmic phase and  $\gamma_R=2688s^{-1}$  just before the disruption. The latter value corresponds to a very low stability margin and, consequently, we are close to the maximum elongation at  $I_p=300kA$ .

The discharge stability was improved by reducing the injected power to 1MW and moving the ECH deposition out during the elongation process. This allowed completely stable non-disruptive discharges at  $\kappa=2.4$ , Fig. 5, with  $\gamma_R=2238s^{-1}$  at the highest elongation,  $t=1.4s$ . The lower beam is moved out (Fig. 5b) during the discharge to keep the deposition location

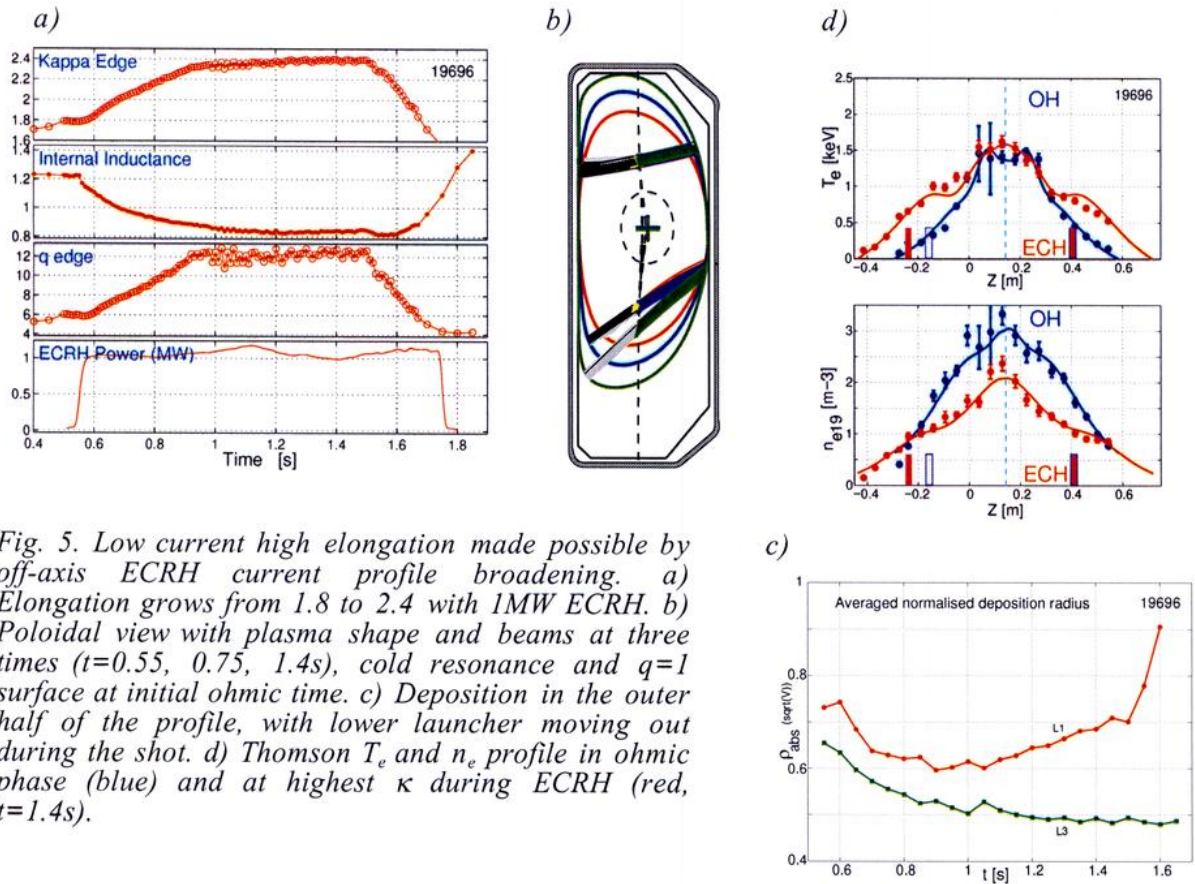


Fig. 5. Low current high elongation made possible by off-axis ECRH current profile broadening. a) Elongation grows from 1.8 to 2.4 with 1MW ECRH. b) Poloidal view with plasma shape and beams at three times ( $t=0.55, 0.75, 1.4s$ ), cold resonance and  $q=1$  surface at initial ohmic time. c) Deposition in the outer half of the profile, with lower launcher moving out during the shot. d) Thomson  $T_e$  and  $n_e$  profile in ohmic phase (blue) and at highest  $\kappa$  during ECRH (red,  $t=1.4s$ ).

approximately constant at  $\rho_{dep} \sim 0.7$  (Fig. 5c), which allows a more economical use of the deposited power while elongating. The ECH power was shut off only after the pre-programmed elongation ramp-down, permitting a soft termination of the discharge. The electron temperature profile is broadened, with a distinct shoulder at the power deposition location, see Fig. 5d top. The density profile is strongly modified with a pump-out effect removing density from the deposition location, pushing it to the centre and to the edge. This explains strong density peaking on axis and a high gas injection rate to compensate for the outward flux. A power balance analysis shows that the heat flux and the electron conductivity  $\chi_e$  is strongly reduced to values below the ohmic level inside the deposition radius and increased outside.

Soon after the heating starts, the central  $q_0$  moves above unity and sawteeth disappear. Due to the  $\rho_{dep}$  sweep during the discharge and the induced  $q$ -profile change, the power deposition location crosses integer- $q$  surfaces. However no deleterious MHD was noticed in these high  $q$

discharges. The final elongation depends only weakly on power. It also depends weakly on the location of the power deposition as long as the deposition occurs in the outer half of the profile.

However, there is an outer limit for the initial deposition radius beyond which the first-pass absorption is too low to embark on an elongation process. A successful elongation run was still obtained with 2MW and starting the deposition as far out as  $\rho \sim 0.8$ , with a first-pass absorption below 50% ( $n_{e19} \sim 0.7$ ,  $T_e \sim 0.3\text{keV}$  at the absorption layer). Lowering the power to 1MW required a more central initial deposition location.

#### 4. Conclusion

In the experiments with central heating inside  $q=1$ , the observed sawtooth period has been successfully used to link the experiment with the Mercier ideal stability criterion and with internal kink stability. The scans in plasma shape in TCV have allowed: 1) the experimental determination of the effect of plasma shape and central pressure on sawtooth stability, 2) the demonstration of the contribution of the ideal internal kink mode in triggering the sawtooth crash at high elongation and at low triangularity [1]. In ohmic discharges, the sawtooth period and amplitude continue to decrease when the elongation increases up to an elongation  $\kappa \sim 2.3$ -2.6 or down to a low inductance limit, where the sawteeth abruptly disappear below resolution. The  $q=1$  radius and the flat temperature profile inside  $q=1$  remain unchanged throughout this transition, which suggests that there is still a physical mechanism at work flattening the core profile at extreme elongation, even though sawteeth are no more observable.

Far off-axis second harmonic X-mode ECH power deposition proves to be an efficient tool for current profile tailoring allowing a significant elongation increase at fixed quadrupole field. The operation at low current and high elongation has been substantially extended with off-axis ECH current profile broadening, making low current operation possible at current densities 2.5 times lower than in similar ohmic plasmas. From the present experience, stable high elongation discharges at  $\kappa > 2.4$  will require higher currents, since the axi-symmetric growth rate reached in the present experiments is close to the limit. Furthermore, the exploitation of the high  $\beta$  potential of elongated discharges would require a normalised current around  $I_N = I/aB \sim 2.0\text{MA/mT}$ , a factor of 2 above the  $0.84\text{MA/mT}$  achieved here. This opens a new area for confinement and stability limit studies at high elongation, e.g. combining second harmonic (X2) current profile broadening and third harmonic (X3) central heating [17].

**Acknowledgement:** This work was partly supported by the Swiss National Science Foundation.

#### References:

- [1] REIMERDES H., POCHELON A., SAUTER O., GOODMAN T.P., HENDERSON M.A., MARTYNOV A.A., Plasma Phys. Contr. Fusion **42** (2000) 629.
- [2] HOFMANN F., SAUTER O., REIMERDES H., FURNO I., POCHELON A., Phys. Rev. Lett. **81**, (1998) 2918.
- [3] GOODMAN T.P., ALBERTI S., HENDERSON M.A., POCHELON A., TRAN M.Q., 19th Symp. on Fusion Technology, Lisbon, Portugal, 1996, Vol. I (1996) 565.
- [4] LÜTJENS H., BONDESON A. and VLAD G., Nucl. Fusion **32** (1992) 1625.
- [5] DEGTYAREV L., MARTYNOV A., MEDVEDEV S., TROYON F., VILLARD L., GRUBER R., Comput. Phys. Commun. **103** (1997) 10.
- [6] PORCELLI F., BOUCHER D. and ROSENBLUTH M.N., Plasma Phys. Contr. Fus. **38** (1996) 2163.
- [7] MARTYNOV A. and SAUTER O., Proc. of Theory of Fusion Plasmas, Varenna 2000, ISSP-19 (Editrice Compositori, Bologna, 2001) 387.
- [8] DUPERREX P.A., POCHELON A., EDWARDS A.W., SNIPES J.A., Nucl. Fusion **32** (1992) 1161.
- [9] GUITTIENNE Ph., Private communication (1996).
- [10] POCHELON A., GOODMAN T.P., HENDERSON M.A. et al., Nucl. Fus. **39**, No.11Y (1999) 1807.
- [11] TFR-GROUP, Proc. 6th Int. Conf. on Plasma Phys. and Contr. Nucl. Fus. Research, Berchtesgaden Vol. I (1976) 279.
- [12] SIMM W., Thesis, Lausanne Laboratory Report LRP 334/87 (1987).

- [13] ANGIONI C., GOODMAN T.P., PIETRZYK Z.A., SAUTER O., Proc. of Theory of Fusion Plasmas, Varenna 2000, ISSP-19 (Editrice Compositori, Bologna, 2001) 73.
- [14] BOUCHER D. and REBUT P.H., in Proc. IAEA Tech. Com. on Advances in Simulation and Model. of Thermonuclear Plasmas, 1992, Montreal (1993) 142.
- [15] REBUT P.H., LALLIA P.P. and WATKINS M.L., Proc. 12th Int. Conf. Plasma Physics and Controlled Nuclear Fusion Research, Nice 1988, IAEA Vienna 1989, Vol. 2, 191.
- [16] HOFMANN F., MORET J.-M., WARD D.J., Nuclear Fusion **38** (1998) 1767.
- [17] ALBERTI. S. et al., Proc. 18th IAEA Fusion Energy Conf., Sorrento 2000, paper PD/2.